Deciphering the scopolamine challenge rat model by preclinical functional MRI

Gergely Somogyi[1#], Dávid Hlatky[1#], Tamás Spisák[1, 2], Zsófia Spisák[1], Gabriella Nyitrai[1], András Czurkó[1*]

[#]These authors contributed equally to this work.

[1] Preclinical Imaging Center, Pharmacology and Drug Safety Research, Gedeon Richter Plc., Budapest, Hungary

[2] Department of Diagnostic and Interventional Radiology and Neuroradiology, University Hospital Essen, Essen, Germany

[*]Corresponding author:

András Czurkó

Pharmacology and Drug Safety Research

Gedeon Richter Plc.,

POB: 27, Budapest 10, H-1475,

Hungary.

Tel.: +36 1 431 5870;

fax: +36 1 505 7275.

E-mail address: czurkoa@richter.hu

Abstract

Systemic administration of cholinergic antagonist scopolamine (SCO) is a widely used model to induce experimental cognitive impairment during preclinical drug testing of putative procognitive compounds. This model, however, has limited predictive validity partly due to its peripheral side-effects, therefore objective neuroimaging measures would greatly enhance its translational value. To this end, we administered SCO and peripherally acting butylscopolamine (BSCO) in preclinical functional MRI (fMRI, 9.4T) studies and measured their effects on whisker stimulation induced fMRI activation in Wistar rats. Beside the commonly used gradient echo echo-planar imaging (GE EPI) an arterial spin labeling method was also used to elucidate the vasculature-related properties of the BOLD-response. To account for anesthesia-effects, in two separate experiments we used isoflurane and combined (isoflurane + i.p. dexmedetomidine) anesthesia. In the second experiment with GE EPI and spin echo (SE) EPI sequences the effect of donepezil (DON) was also examined. In isoflurane anesthesia with GE EPI, SCO decreased the evoked BOLD response in the barrel cortex (BC), while BSCO increased it in the anterior cingulate cortex. In the combined anesthesia SCO decreased the activation in the BC as well as in the inferior colliculus (IC) while BSCO reduced the response merely in the IC. Our results revealed that SCO attenuated the evoked BOLD activation in the BC as a probable central effect in both experiments while its other detected actions depended on the type of anesthesia or dose and the given fMRI sequences.

Introduction

On the bases of the cholinergic hypothesis of geriatric memory dysfunction [1] scopolamine became a standard reference drug for inducing experimental cognitive impairment in both animals and humans [2-4]. The so called "scopolamine challenge" is widely used in preclinical testing of new substances for putative procognitive compounds [5-7]. This approach, i.e. the reversal of scopolamine-induced impairments, however, has limited predictive validity as it tends to yield a high number of false positives [8,9]. Specifically, one of the important limitations of the scopolamine (SCO) model is, its peripheral side-effects that can influence the learning and memory deficits observed at higher doses of SCO [4].

In contrast on the basis of its peripheral vascular action as a primary mechanism, a SCO provocation-based pharmaco-MRI model was proposed as a test for procognitive agents [5,10]. Indeed, non-blood-brain barrier-penetrating anticholinergic drug, butylscopolamine (BSCO) also evoked learning deficit similarly to SCO and both compounds induced negative blood oxygen-level-dependent (BOLD) changes in the prefrontal cortex in a pharmaco-MRI study, in isoflurane anesthesia [10]. However, in α-chloralose anesthesia in a similar preclinical pharmaco-MRI study, the SCO i.v. injection increased the BOLD contrast in the frontal (orbital) cortex and olfactory nuclei while it was absent after BSCO injection [11]. These diverging results highlight the difficulty interpreting preclinical pharmaco-MRI data [12] complicated by the use of different anesthetic regimes [13] that can introduce potential confounds [14].

As MRI acquisition parameters could influence the different signal components of BOLD [15], contrasting gradient echo (GE), spin echo (SE) echo-planar imaging (EPI) and functional arterial spin labeling (ASL) could address interpretation issues and provide a deeper insight into the SCO model. Likewise, performing functional MRI measurements in a block-design in different anesthetic regimes could yield useful, translatable information for the SCO challenge in preclinical drug testing efforts.

Therefore, in the present study, we measured whisker stimulation induced BOLD activation and the effect of SCO in two experiments on an ultrahigh field (9.4T) preclinical MRI system in rats. In the first experiment SCO and peripherally acting analogue BSCO were used as a pretreatment and BOLD activation were measured to air puff stimulation of the whisker pad with GE echo planar imaging (EPI) sequence in isoflurane anesthesia and with functional ASL in the same measurement.

In the second experiment, SCO and BSCO were used in combined i.p. medetomidine + isoflurane anesthesia and additionally the effect of cholinesterase inhibitor donepezil (DON) was examined on the whisker stimulation evoked BOLD response with both GE EPI and SE EPI sequences.

Materials and methods

Animals

Thirty-four drug-naïve adult male Wistar (RJ Han, Harlan Laboratories (Envigo)) rats were used for the two experiments (Exp.1: *n*=18; Exp.2: *n*=16,). The animals were kept by controlled laboratory conditions (constant temperature and humidity) in polycarbonate cages under standard in a 12h light/dark cycle with light on at 6:00 a.m. The rats were fed with conventional laboratory rat food (sniff R/M + H Spezieldiäten GmbH D-59494 Soest), with food and water ad libitum. All the procedures conformed to the guidelines of the National Institutes of Health for the care and use of laboratory animals and were approved by the local Ethical Committee of Gedeon Richter Plc. and were carried out in strict compliance with the European Directive 2010/63/EU regarding the care and use of laboratory animals for experimental procedures. All efforts were made to minimize the number of animals as well as pain or discomfort.

Experimental design and drug treatments

The effect of drug pretreatments on the functional MRI activity was examined in a pseudo-randomized cross-over design such that equal numbers of animals received each drug of the given experiment on any given measurement day. There was a minimum interval of seven days between repeated measurements of the same animal. For the average weight of the animal groups see Supplementary Materials and Methods (Table S1, S2).

In experiment 1 (Exp.1), conscious animals received saline (2 ml/kg) or SCO (scopolamine hydrobromide, Tocris) or BSCO (Scopolamine N-butyl bromide, Sigma Aldrich) as pretreatment 1 hour before the start of the MRI measurement. SCO or

BSCO were dissolved in distilled water or saline, respectively, and injected intraperitoneally at a dose of 0.3 mg/kg.

In experiment 2 (Exp.2), conscious animals received saline (2 ml/kg), SCO (1 mg/kg), BSCO (1 mg/kg) or DON (Donepezil hydrochloride, 71078800, L77028F, Gedeon Richter Plc.). DON was dissolved in distilled water and was injected at a dose of 3 mg/kg.

Anesthesia during the fMRI scanning

In Exp.1 after the drug pretreatment animals were anesthetized with 5% isoflurane (Forane, Abbot Laboratories) and then maintained at approximately 1.25% during scanning. Other part of the scanning procedure was identical to the procedures outlined previously [16-18]. In Exp.2 the anesthesia was introduced with a bolus of medetomidine injection (0.05 mg/kg i.p. dexdor, dexmedetomidine, Orion Pharma) plus 5% isoflurane in air and the concentration of isoflurane was lowered to 0.25% - 1.5% during scanning with the aim of keeping the respiration rate near 60/min. For mean isoflurane dose of the animal groups see Supplementary Materials and Methods (Table S1, S2).

Image acquisition

The MRI experiments were performed on a 9.4 T Varian (Agilent) Direct Drive MRI system (Varian Medical Systems Inc., Palo Alto, CA). MRI system parameters described in detail previously [16-18], also see Supplementary Materials and Methods.

Anatomical images for the fMRI registration were proton density (PD) weighted gradient-echo multi-slice imaging (GEMS) in horizontal orientation, and/or a T2 weighted fast spin-echo multi-slice imaging (FSEMS) anatomical scans in axial orientation, see Supplementary Materials and Methods.

BOLD fMRI EPI sequences

Echo planar imaging (EPI) sequences were used for the BOLD measurements. Gradient echo EPI (GE EPI: TR/TE = 1000ms/10ms, FA: 90°) and spin echo EPI (SE EPI: TR/TE = 1000ms/40ms, FA: 90°) sequences were used (Supplementary Materials and Methods).

ASL fMRI sequence

For multislice arterial spin labeling (ASL) measurements a flow-sensitive alternating inversion recovery (FAIR-ASL, TR/TE = 3.6s/18ms, matrix: 64×64, slice thickness: 2mm, 9 axial slices) sequence was used as described by Nashrallah et al. in [19], see Supplementary Materials and Methods.

Whisker stimulation

During the functional MRI experiments, whisker stimulation by air puffs was used in a block-design fashion. The stimulation procedure was identical to the procedure outlined previously [16-18]. The duration of one stimulation block was 30 s followed by 60 s rest and one measurement session contained 6 blocks in case of the GE-EPI and SE-EPI BOLD fMRI measurements with an initial 120 s resting. For ASL-BOLD fMRI, a 36-72 s on-off cycle was used. See Supplementary Materials and Methods for details.

Data analysis

Throughout the image processing procedure, we intended to follow the conventional human- research practice in fMRI analysis. The analysis was carried out in a multistage process using the image analysis software package, FSL [20] (FMRIB's Software Library, www.fmrib.ox.ac.uk/fsl) and in-house developed software tools. Small-animal imaging specific details of the applied image processing pipeline were described in detail previously [16-18]. The present data analysis is detailed in Supplementary Materials and Methods in section Data analysis.

Functional MRI analysis

Data processing for functional images (GE EPI, SE EPI and ASL –see also Supplementary Materials and Methods) were carried out using FSL FEAT in order to investigate the effects of treatment groups and their differences. Gaussian kernel (for spatial smoothing and high-pass temporal filtering was applied. After signal prewhitening, the first-level statistical analysis was carried out using the general linear model with local autocorrelation correction [21]. The analysis -block design convolved with HRF- modelled each individual rat's data from each session and included 5 noise-ROI-based CompCor [22] confounder variables. Individual statistical Z-score images for the BOLD regressor-of-interest were obtained (average BOLD response to the stimuli). Using the spatial transformations computed during image coregistration and standardization, Z-score maps resulting from the individual statistical analysis were realigned to the common standard space to achieve spatial correspondence during the higher-level analysis.

Fixed-effect group-level statistical analysis was performed on the obtained z-stats using FSL FEAT for voxelwise inference using Gaussian random field (GRF) theory based maximum height thresholding with a (corrected) significance threshold of P=0.05 [23]. Similarly, clusterwise thresholding with a corrected significance threshold of P=0.05 at a cluster-forming threshold of p=0.001 (Z>3.1) was performed. This thresholding method was used to enhance the detection of large activation clusters unlikely to be random false positives originating from multiple comparisons [24]. Furthermore, we applied the probabilistic threshold-free cluster enhancement (pTFCE) [25] with corrected significance threshold of P=0.05. pTFCE provides a natural adjustment for various signal topologies (thereby enhanced P-values directly, without permutation testing). The method is able to detect spatially extended but relevant signals of low magnitude, as well as small activations, which remain hidden with the robust, but often too conservative voxelwise statistics. This method was implemented in R software (The R Project for Statistical Computing, https://www.r-project.org).

Results

The whisker stimulation evoked BOLD activation in the barrel cortex (BC) was variable in size and depended on the anesthesia and MRI sequences. Overview of the experiments are shown in Fig. 1 and Table S3.

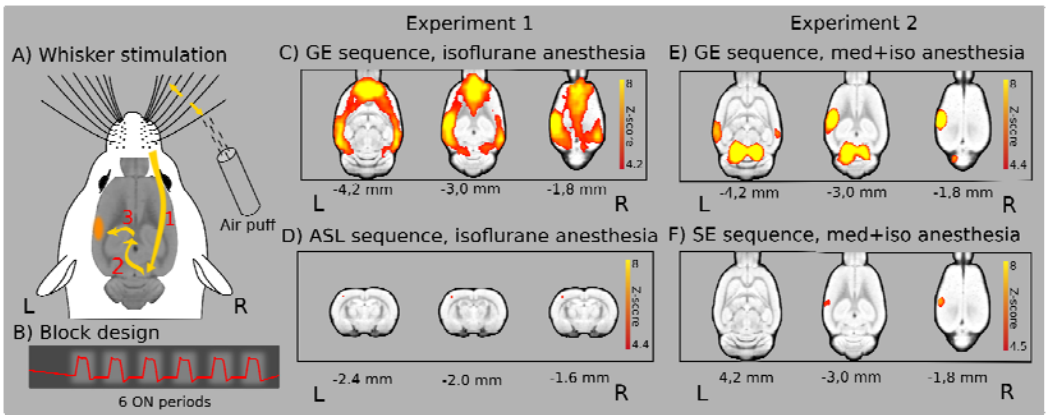

Fig. 1. Air puff stimulation of the right whisker pad in experiment 1 and 2. **a** Signal path from whisker stimulation to activation in the barrel cortex ((1) trigeminal nerve, brain stem, (2) sensory information to the thalamus, (3) the primary somatosensory barrel cortex (BC)). **b** Block-design of whisker air puff stimulation. **c** Widespread cortical BOLD activation in isoflurane anesthesia with gradient-echo (GE) EPI sequence. **d** Limited activation detected in the BC with the ASL sequence in the same experiment. **e** Pronounced activation in the left BC and in the IC bilaterally in the combined anesthesia. **f** Limited activation in the BC with the SE sequence in the same experiment. The Z-scores represent voxelwise statistical inference ($p<0.05$ correcting for multiple comparison via GRF theory based FWER). The corresponding colorbars are depicted on the right. The z (or y) coordinates (distance from Bregma) are given below the slices (L and R stands for directions).

For weights, average in-scanner motions, isoflurane doses and respiration rates see Supplementary Materials and Methods (Table S1, S2). These data show that neither of these variables had any effect that related to the applied treatment in either experiment.

Whisker stimulation evoked BOLD responses in isoflurane anesthesia with gradient-echo (GE) EPI sequence

In experiment 1 air puff stimulation of the right whisker pad evoked widespread cortical BOLD activation in all three treatment groups (Fig. 1, Fig. S1 and Table S3). In the saline (Sal) group, the strongest activation peak was found in the left primary somatosensory cortex, barrel field (L S1 BF). The activation extended bilaterally to wide cortical areas, rostrally it involved the orbital, infralimbic, prelimbic and cingulate cortices, and caudally the auditory, posterior parietal, visual, perirhinal and retrosplenial cortices. For the SCO and BSCO group activations see Fig. S1 and Table S3. For the analysis with three different statistical inferences (voxel, cluster, pTFCE) see Table S4. For local maxima and signal changes with voxelwise statistical inference see Table S5.

Treatment group differences in isoflurane anesthesia with GE EPI sequence

Between-group fMRI contrasts revealed statistically significant differences of the groupwise activation patterns between the treatment groups (Fig. 2, Table S6). The Sal > SCO contrast with voxelwise statistics (Fig. 2a, Table S6) revealed three small areas of statistically significant decreased BOLD response (Fig. 2a, Table S6). The two larger blobs were in the L S1 BF and in the left primary visual cortex, monocular area (L V1 M). With clusterwise statistics, an additional larger blob in the right primary somatosensory cortex, forelimb region (R S1 FL) was found (Fig. 2a, Table S6). With pTFCE (GRF corrected (4.7 < z)) statistics, three additional blobs were significant beside the L V1 M, the secondary somatosensory cortex (R S2), the presubiculum (L PrS) and the primary auditory cortex (R Au1, Fig. 2a, Table S6).

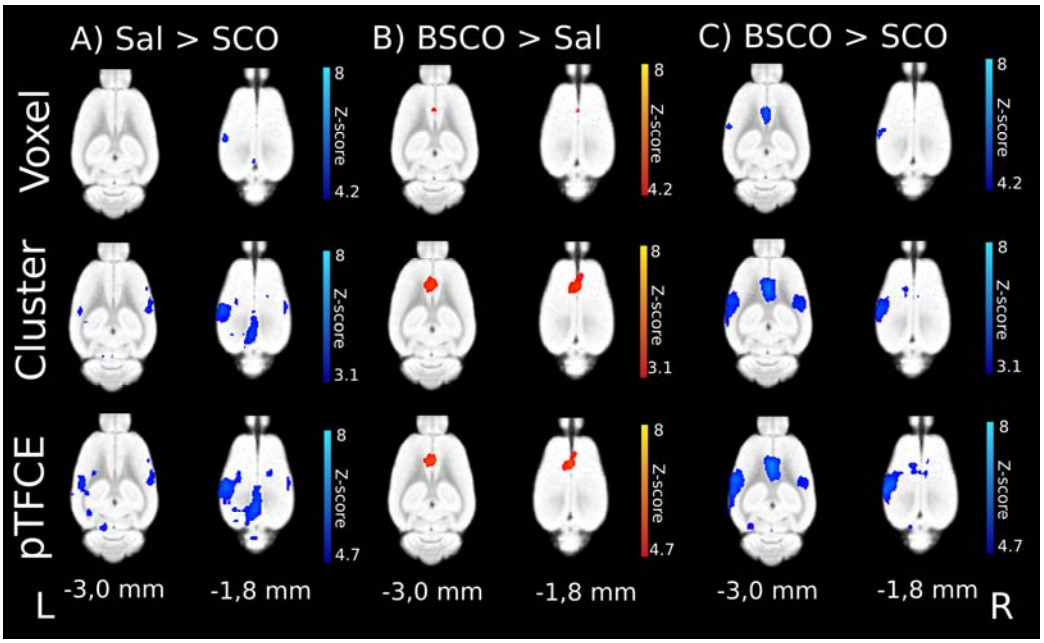

Fig. 2 Evoked BOLD response differences between groups with GE EPI sequence in isoflurane anesthesia. **a** Decreased BOLD response in the scopolamine (SCO) treated group compared to saline (Sal > SCO). **b** Increased BOLD response in the butylscopolamine (BSCO) group compared to saline (BSCO > Sal). **c** Differences between the SCO and BSCO treated groups (BSCO > SCO). The Z-scores in the upper row (Voxel) represent voxelwise statistical inference ($p<0.05$ correcting for multiple comparison via GRF theory based FWER, navy blue-to-light blue or red-to-yellow from $z=4.2$ to $z=8$); in the middle row (Cluster) clusterwise statistical inference ($p<0.05$ correcting for multiple comparison via GRF theory based FWER and a cluster forming threshold of $p=0.001$, navy blue-to-light blue or red-to-yellow $z=3.1$ to $z=8$); in the lower row probabilistic TFCE (pTFCE) statistics ($p<0.05$ correcting for multiple comparison via GRF theory based FWER, navy blue-to-light blue or red-to-yellow $z=4.7$ to $z=8$) from the same data. The corresponding colorbars are depicted on the right. The z coordinates (distance from Bregma) of the selected slices (-3.0 mm; -1.8 mm) are given at the bottom of the figure (L, R stands for directions).

In the SCO > Sal contrast only the uncorrected pTFCE ($3.1 < z$) statistics revealed a difference in the cingulate cortex (L Cg1, Table S6). In the BSCO > Sal contrast all statistics (Fig. 2b, Table S6) revealed significant difference in the cingulate cortex (L Cg2 or Cg1, Table S6).

In the BSCO > SCO contrast the combination of the Sal > SCO and BSCO > Sal contrasts appeared. Voxel level statistics revealed differences in the L S1 BF and L Cg2. Cluster level statistics additionally revealed the R S1 BF and the pTFCE (GRF corrected ($4.7 < z$) revealed three additional ones (Fig. 2c, Table S6).

In the Sal > BSCO and SCO > BSCO contrasts there were no significant differences with clusterwise statistics. For the voxelwise and pTFCE statistics see Supplementary Table (Table S6).

Whisker stimulation evoked responses with functional ASL sequence in isoflurane anesthesia

Whisker stimulation induced activations were focal with the ASL sequence. The combined effect of Sal, SCO and BSCO induced small, focal activations in the L S1 BC and in the L ECIC (Fig. S2) with clusterwise statistical inference. In the L BC significant blobs were appeared in the Sal (as shown also in Fig. 1) and BSCO treatment groups (this effect was visible with the voxelwise and GRF corrected pTFCE statistic as well), but in SCO this focal activation could only be detected by the uncorrected pTFCE (3.1 < z) inference. These statistical results are explicable with the signal changes in the masked L S1 BF as shown in Fig. S2. The uncorrected pTFCE (3.1 < z) statistics detected the L S1 BF in the SCO group (Fig. S3 and Tables S7), but there were additional smaller activations in the left inferior colliculus and retrosplenial cortex (Tables S7). Between-group fMRI analysis of the groupwise activation patterns revealed no statistically significant differences between the treatment groups. For the effect of the treatment groups on signal changes during functional ASL measurements and the difference between the tagged and non-tagged ASL images over time see Supplementary Fig. S4 and Fig. S5.

Whisker stimulation evoked BOLD responses in medetomidine-isoflurane combined anesthesia with the GE EPI sequence

In this measurement the whisker stimulation induced BOLD activations had a characteristic focal appearance (Fig. 1) in all four treatment groups (Fig. S6 and Tables S8). In the Sal group, with voxelwise statistical inference, the strongest activation peaked in the left external cortex of inferior colliculus (L ECIC) but the large activation area bilaterally involved the inferior colliculus (IC) and extended rostrally, bilaterally to medial geniculate nucleus and on the left, to the ventral

posteromedial thalamic nucleus (VPM). A second large activation area peaked in the L S1 BF that also extended to the left auditory cortex and temporal association cortex. The third smaller activation area peaked in the right primary auditory cortex (R Au1).

In the SCO and BSCO groups (1.0 mg/kg) the whisker stimulation induced activation patterns were very similar to the Sal group (Fig. S6 and Tables S8). In the DON group the same activation pattern was seen but the activations were somewhat smaller (Fig. S6 and Tables S8).

Treatment group differences in medetomidine-isoflurane combined anesthesia with the GE EPI sequence

Between-group fMRI analysis contrasts revealed significant differences in this measurement (Fig. 3, Table 1). In the Sal > SCO contrast the voxelwise statistical inference revealed decreased activation due to SCO in the L ECIC and the L S1 BF while clusterwise statistics highlighted only the L ECIC (Table S10). The pTFCE statistics (GRF corrected (4.7 < z)), detected the L ECIC and one voxel in the L S1 BF while the uncorrected pTFCE (3.1 < z) statistics detected a larger blob in the L S1 BF and the left and right ECIC (L & R ECIC, Table 1).

In the Sal > BSCO contrast voxelwise and pTFCE (GRF corrected (4.7 < z)) statistics revealed a statistically significant decreased BOLD response due to BSCO in the L ECIC (Table 1 and Table S10).

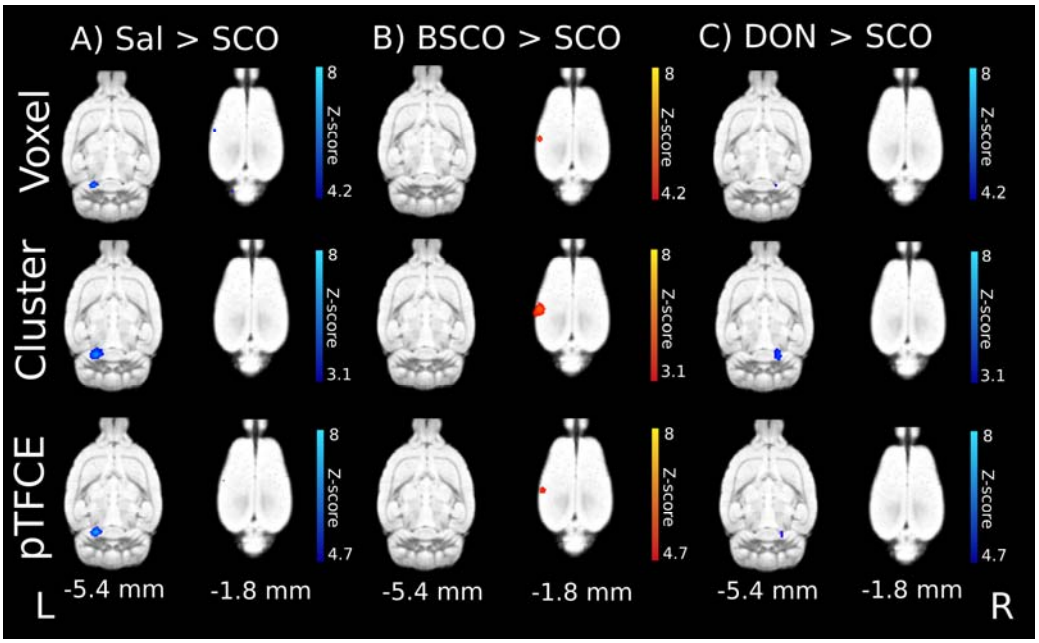

Fig. 3 Evoked BOLD response differences between groups with GE EPI sequence in medetomidine-isoflurane combined anesthesia with GE EPI sequence. **a** Sal > SCO contrast. **b** BSCO > SCO contrast. **c** DON > SCO contrast. Decreased BOLD responses in the BC due to SCO (**a, b**) and in the IC due to both SCO (and BSCO; **a, b**). Decreased BOLD responses in the left IC in the DON > SCO contrasts(**c**). The Z-scores in the upper row (Voxel) represent voxelwise statistical inference ($p<0.05$ correcting for multiple comparison via GRF theory based FWER, navy blue-to-light blue or red-to-yellow from z=4.2 to z=8); in the middle row (Cluster) clusterwise statistical inference ($p<0.05$ correcting for multiple comparison via GRF theory based FWER and a cluster forming threshold of p=0.001, navy blue-to-light blue or red-to-yellow z=3.1 to z=8); in the lower row probabilistic TFCE (pTFCE) statistics ($p<0.05$ correcting for multiple comparison via GRF theory based FWER, navy blue-to-light blue or red-to-yellow z=4.7 to z=8) from the same data. The corresponding colorbars are depicted on the right. The z coordinates (distance from Bregma) of the selected slices (-5.4 mm; -1.8 mm) are given at the bottom of the figure (L, R stands for directions). In the Sal > DON contrast only the clusterwise and uncorrected pTFCE (3.1 < z) statistics revealed a difference in the left cerebellar lobe (IC) due to the 3.0 mg/kg DON (Table 1 and Table S10).

In the BSCO > SCO contrast all statistics revealed a difference in the L S1 BF (Fig. 3, Table 1 and Table S10). Likewise comparing the Sal > SCO and Sal > BSCO contrasts, it

might suggest that in this measurement in the L ECIC could be a peripheral effect (Fig. 3 and Table 1).

In both the DON > SCO and DON > BSCO contrasts there were significant differences in the R ECIC area with all statistics (Fig. 3 and Table 1 and Table S10).

In the SCO > Sal, SCO > BSCO, SCO > DON and BSCO > Sal contrasts only the uncorrected pTFCE (3.1 < z) statistics found differences (Table 1 and Table S10).

In the BSCO > DON and DON > Sal contrasts there were no differences with either statistics (Table S10).

Whisker stimulation evoked BOLD responses in medetomidine-isoflurane combined anesthesia with SE EPI sequence

In this measurement the whisker stimulation induced BOLD activations were focal and localized to the L S1 BF in all four treatment groups (Fig. S7 and Table S9).

Treatment group differences in medetomidine-isoflurane combined anesthesia with the SE EPI sequence

Between-group fMRI contrasts revealed significant activation differences only with pTFCE statistics in this measurement, (Table 1). In the BSCO > SCO contrast, with the pTFCE (GRF corrected (4.7 < z)) statistics only one voxel difference was found in the L S1 BF. This one voxel difference also mirrored in the L S1 BF in the DON > SCO and DON > BSCO contrasts (Fig. 4 and Table 1). The uncorrected pTFCE (3.1 < z) also revealed these and other differences in the majority of contrasts (Table 1 and Table S10).

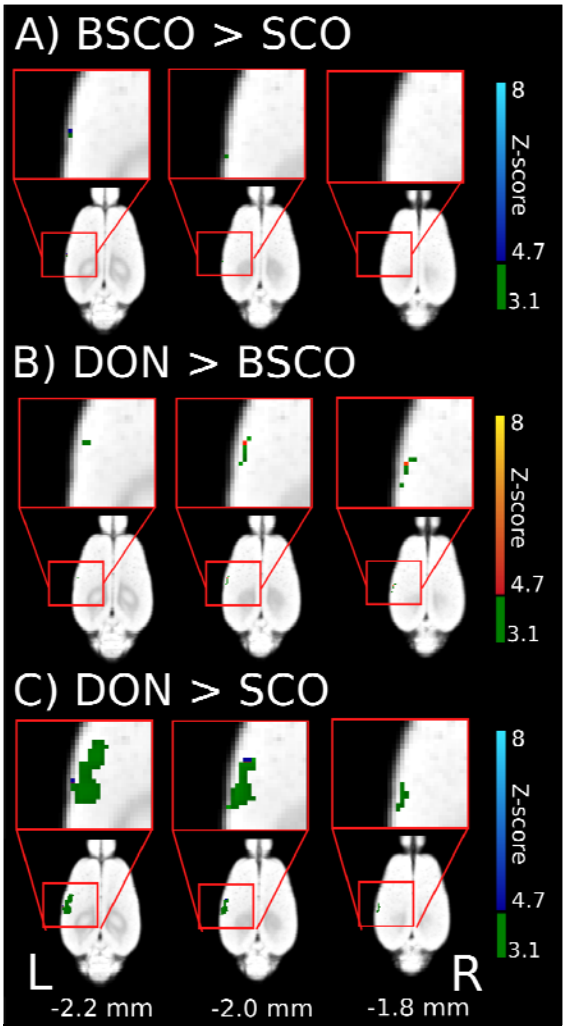

Fig. 4 BOLD response differences with the SE EPI sequence between treatment groups in medetomidine-isoflurane combined anesthesia: BSCO > SCO (**a**); DON > BSCO (**b**); DON > SCO (**c**) contrasts. **a, b** In the BSCO > SCO and DON > BSCO contrasts only one-one voxel difference was found in the left somatosensory cortex, barrel field (L S1 BF) with the pTFCE (GRF corrected (4.7 < z)) statistical inference. **c** In the DON > SCO BOLD contrast with the SE EPI sequence the corrected pTFCE (GRF corrected (4.7 < z)) statistics revealed 3 voxels and the uncorrected pTFCE (green, 3.1 < z) revealed a larger area in the L S1 BF. Corresponding colorbars show the pTFCE statistical inference: green (uncorrected) from z=3.1 to z=4.7, red-to-yellow or navy blue-to-light blue (corrected) from z=4.7 to z=8. The z coordinates (distance from Bregma) of the selected slices (-2.2 mm, -2.0 mm, -1.8 mm) are given at the bottom (the L and R stands for the left and right directions).

Discussion

The muscarinic cholinergic antagonist SCO is frequently used to model various aspects of cognitive dysfunction during early drug development [6]. Recently though, the facilitation of motivated behavior was demonstrated by SCO that was able to rescue antipsychotic-induced motivational impairments [26]. An important aspect of the "SCO challenge" model is, that it could also result in an increased release of acetylcholine in the brain by blocking presynaptic muscarinic receptors. This, through the excessive activation of nicotinic receptors, may also mediate the negative effects of SCO on memory [27].

The validity of the SCO induced pharmacological model for cognitive impairment has been reviewed by Klinkenberg & Blokland, concluding important limitations that influence the learning and memory deficits observed at higher doses of SCO. These deficits are most likely mediated by effects on attention and sensory discrimination, non-specific behavioural effects and peripheral side-effects [4].

To advance these preclinical efforts, we thought that objective neuroimaging measures on the "SCO challenge" model would greatly enhance our understanding and its translational value.

Several human fMRI studies, using various memory and attentional paradigms, demonstrated decreased regional CBF and attenuation in the memory-task-induced increases of regional CBF and BOLD activation after SCO in various frontal brain areas [28-32].

While the acute i.v. administration of SCO in humans produces a deficit in frontal cortical perfusion [33], it also produces a transient reduction of the heart rate and blood pressure [34]. The acute i.v. SCO infusion could transiently enhance the putative central parasympathetic autonomic outflow, and this could interfere with the neuroimaging data described above [35].

Therefore, to avoid the transient effects of SCO, we did not use the traditional preclinical pharmaco-MRI approach with acute i.v. anticholinergic infusion but a

“task” fMRI with a pretreatment (1 hour). This pretreatment is similar to those behavioural studies where SCO is used to induce cognitive impairment[36]. We used the preclinical MRI as a “task” fMRI, by measuring the whisker stimulation induced BOLD activation in a block design. With this approach, we could not see the dramatic reduction of perfusion or negative BOLD in the prefrontal cortex that would explain some behavioral effects [5,10,33].

Interestingly, in a previous perfusion imaging study with similar SCO pretreatment (1 hour) an increased rCBV was found in young dogs, unexpectedly [37]. Furthermore, a SCO induced hyperactivation was also reported in the frontal and prefrontal cortical areas during a working memory-task [38].

In experiment 1, in isoflurane anesthesia with GE EPI sequence, the whisker stimulation evoked a widespread cortical BOLD activation and group differences revealed a decreased BOLD response in the barrel cortex (BC) due to SCO. Interestingly, BSCO increased the evoked BOLD response in the anterior cingulate cortex (Cg1). The SCO result is in line with the human fMRI studies where the SCO attenuated the evoked BOLD activation while the BSCO result would mark a peripheral effect in the BOLD activation contrast.

In experiment 1, in the ASL-BOLD measurement the whisker stimulation of the combined effect of Sal, SCO and BSCO induced small, focal activations in the L BC and in the L ECIC (Fig. S2) with clusterwise statistical inference. In the L BC are appeared significant blobs in the Sal and BSCO treatment groups, but in SCO this focal activation could only be detected by the uncorrected pTFCE ($3.1 < z$) inference. The apparent difference in activation maps between the GE EPI and ASL sequences may be due to the differences in their signal to noise ratio but the GE EPI sequence is also more sensitive to the intra- and extravascular effects of BOLD which also appears in the response differences between treatment groups, consequently for the larger pial surface veins and possibly to the peripheral effects of drugs.

Exp. 1 was done in isoflurane anesthesia that is ideal to perform non-invasive longitudinal studies [16-18,39,40]. There is a chance however, that isoflurane itself

could interfere with the cholinergic system [41,42], although it lacks functional groups and only interact with its targets through weak polarization force [43,44]. On the other hand, isoflurane may weaken the blood-brain barrier [45] by modulating tight junction protein expression [46], that may influence the effect of BSCO in our study.

Furthermore, isoflurane anesthesia may induce neurophysiologically defined propagating slow calcium waves, that reflected in pan-cortical BOLD fMRI activation [47]. This may explain the widespread cortical BOLD activation evoked by the whisker stimulation with GE EPI sequence in isoflurane anesthesia in Exp. 1. To address some of the above issues, in Exp. 2 we used combined medetomidine-isoflurane anesthesia and higher doses of our drug pretreatments. Here the same whisker stimulation evoked characteristic focal BOLD activations with the GE EPI sequence that involved the left BC and bilaterally the central nuclei of the inferior colliculus (IC). This profound bilateral activation of the IC is an unexpected finding, although the strong background acoustic noise of the scanner is always present. Our fMRI measurement used whisker stimulation in block design, thus it may look surprising that a constant background acoustic noise would induce profound activation. It was demonstrated however, that the scanner acoustic noise can modulate the somatosensory stimulation. Specifically, the somatosensory activation was facilitated by the simultaneous acoustic noise [48]. It is also known that the IC receives ascending projections from both auditory and somatosensory nuclei, and it should be regarded as a node in multisensory integration [49,50]. Nonetheless, the profound activation of the IC in the combined medetomidine-isoflurane anesthesia in Exp 2 is still remarkable. Regarding anesthesia, it is also interesting that a PET study of auditory activation also observed significantly higher 18F-FDG uptake in the IC in a combined medetomidine anesthesia compared to another type of anesthesia [51].

Group differences with the GE EPI sequence show that both SCO and BSCO decreased the BOLD activation in the IC (Sal > SCO, Sal > BSCO), while SCO also

decreased the BOLD activation in the BC. In the BSCO > SCO contrast all statistics revealed a difference in the L S1 BF. This may suggest that SCO could decrease the BOLD activation in the L S1 BF as a central effect. Likewise comparing the Sal > SCO and Sal > BSCO contrasts, it might suggest that in this measurement in the L ECIC could be a peripheral effect. In both the DON > SCO and DON > BSCO contrasts there were significant differences in the R ECIC area with all statistics and this difference in the R ECIC might be a peripheral effect.

Therefore, we think that in this measurement both the central (BC) and the peripheral (IC) effects of SCO were observed. Interestingly, in the DON > SCO contrast significant difference in the BC could not be revealed with the GE EPI sequence while differences in some voxels were revealed in the SE EPI measurement by the pTFCE statistical inference.

Our study attempted to preclinically decipher the neuroimaging correlates of the SCO challenge with different statistical inferences. We revealed that the SCO attenuated the evoked somatosensory BOLD activation in the BC, independently from the anesthesia while its perceived peripheral action depended on the type of anesthesia, dose and fMRI sequences.

FUNDING AND DISCLOSURE

The study was supported by Gedeon Richter Plc., the Hungarian National Research, Development and Innovation Office (KMOP-1.1.5-08-2009-0001), and the National Brain Research Program (KTIA_NAP_13-1-2013-0001; 2017-1.2.1-NKP-2017-00002). The authors are employees of Gedeon Richter Plc. or were full time employees of that firm at the time the research was performed, otherwise they declare no conflicts of interest.

ACKNOWLEDGEMENT

The authors are grateful for the technical assistance of Pálma Diószegi and Katalin Tóthné Fekete.

AUTHOR CONTRIBUTIONS

G.S., D.H., T.S., Zs.S., G.Ny. and A.Cz. designed the experiments; D.H. performed the data acquisition; G.S., T.S., Zs.S. analysed the data; G.S., D.H., T.S., G.Ny. and A.Cz. interpreted the data for the work. G.S., D.H. and A.Cz. wrote the main manuscript text and G.S. prepared figures. All authors reviewed the manuscript.

REFERENCES

1 Bartus RT, Dean RL, 3rd, Beer B, Lippa AS. The cholinergic hypothesis of geriatric memory dysfunction. Science. 1982;217(4558):408-14.

2 Ebert U, Kirch W. Scopolamine model of dementia: electroencephalogram findings and cognitive performance. Eur J Clin Invest. 1998;28(11):944-9.

3 Flood JF, Cherkin A. Scopolamine effects on memory retention in mice: a model of dementia? Behav Neural Biol. 1986;45(2):169-84.

4 Klinkenberg I, Blokland A. The validity of scopolamine as a pharmacological model for cognitive impairment: a review of animal behavioral studies. Neurosci Biobehav Rev. 2010;34(8):1307-50.

5 Hegedus N, Laszy J, Gyertyan I, Kocsis P, Gajari D, David S, et al. Scopolamine provocation-based pharmacological MRI model for testing procognitive agents. J Psychopharmacol. 2015;29(4):447-55.

6 Lenz RA, Baker JD, Locke C, Rueter LE, Mohler EG, Wesnes K, et al. The scopolamine model as a pharmacodynamic marker in early drug development. Psychopharmacology (Berl). 2012;220(1):97-107.

7 Snyder PJ, Bednar MM, Cromer JR, Maruff P. Reversal of scopolamine-induced deficits with a single dose of donepezil, an acetylcholinesterase inhibitor. Alzheimers Dement. 2005;1(2):126-35.

8 Barak S, Weiner I. Putative cognitive enhancers in preclinical models related to schizophrenia: the search for an elusive target. Pharmacol Biochem Behav. 2011;99(2):164-89.

9 Sarter M. Preclinical research into cognition enhancers. Trends Pharmacol Sci. 2006;27(11):602-8.

10 Kocsis P, Gyertyan I, Eles J, Laszy J, Hegedus N, Gajari D, et al. Vascular action as the primary mechanism of cognitive effects of cholinergic, CNS-acting drugs, a rat phMRI BOLD study. Journal of cerebral blood flow and metabolism : official journal of the International Society of Cerebral Blood Flow and Metabolism. 2014;34(6):995-1000.

11 Cash D, Roberts TJ, Ireland MD, Williams SCR, Hunter JA, Upton N, et al. Visualizing the effects of scopolamine in the rat brain using functional MRI. J Cereb Blood Flow Metab. 2005;25(1_suppl):S366-S66.

12 Spain A, Howarth C, Khrapitchev AA, Sharp T, Sibson NR, Martin C. Neurovascular and neuroimaging effects of the hallucinogenic serotonin receptor agonist psilocin in the rat brain. Neuropharmacology. 2015;99:210-20.

13 Haensel JX, Spain A, Martin C. A systematic review of physiological methods in rodent pharmacological MRI studies. Psychopharmacology (Berl). 2015;232(3):489-99.

14 Petrinovic MM, Hankov G, Schroeter A, Bruns A, Rudin M, von Kienlin M, et al. A novel anesthesia regime enables neurofunctional studies and imaging genetics across mouse strains. Sci Rep. 2016;6:24523.

15 Renvall V, Nangini C, Hari R. All that glitters is not BOLD: inconsistencies in functional MRI. Sci Rep. 2014;4:3920.
16 Nyitrai G, Spisak T, Spisak Z, Gajari D, Dioszegi P, Kincses TZ, et al. Stepwise occlusion of the carotid arteries of the rat: MRI assessment of the effect of donepezil and hypoperfusion-induced brain atrophy and white matter microstructural changes. PloS one. 2018;13(5):e0198265.
17 Spisak T, Pozsgay Z, Aranyi C, David S, Kocsis P, Nyitrai G, et al. Central sensitization-related changes of effective and functional connectivity in the rat inflammatory trigeminal pain model. Neuroscience. 2017;344:133-47.
18 Spisak T, Roman V, Papp E, Kedves R, Saghy K, Csolle CK, et al. Purkinje cell number-correlated cerebrocerebellar circuit anomaly in the valproate model of autism. Sci Rep. 2019;9(1):9225.
19 Nasrallah FA, Lee EL, Chuang KH. Optimization of flow-sensitive alternating inversion recovery (FAIR) for perfusion functional MRI of rodent brain. NMR Biomed. 2012;25(11):1209-16.
20 Jenkinson M, Beckmann CF, Behrens TE, Woolrich MW, Smith SM. Fsl. NeuroImage. 2012;62(2):782-90.
21 Woolrich MW, Ripley BD, Brady M, Smith SM. Temporal autocorrelation in univariate linear modeling of FMRI data. NeuroImage. 2001;14(6):1370-86.
22 Behzadi Y, Restom K, Liau J, Liu TT. A component based noise correction method (CompCor) for BOLD and perfusion based fMRI. NeuroImage. 2007;37(1):90-101.
23 Worsley KJ. Statistical analysis of activation images. In: Jezzard P, Matthews PM, Smith SM, editors. Functional MRI: An Introduction to Methods. Oxford: Oxford Universtiy Press; 2001. p. 251-71.
24 Friston KJ, Worsley KJ, Frackowiak RS, Mazziotta JC, Evans AC. Assessing the significance of focal activations using their spatial extent. Human brain mapping. 1994;1(3):210-20.
25 Spisak T, Spisak Z, Zunhammer M, Bingel U, Smith S, Nichols T, et al. Probabilistic TFCE: A generalized combination of cluster size and voxel intensity to increase statistical power. NeuroImage. 2018;185:12-26.
26 Hailwood JM, Heath CJ, Phillips BU, Robbins TW, Saksida LM, Bussey TJ. Blockade of muscarinic acetylcholine receptors facilitates motivated behaviour and rescues a model of antipsychotic-induced amotivation. Neuropsychopharmacology. 2019;44(6):1068-75.
27 Newman LA, Gold PE. Attenuation in rats of impairments of memory by scopolamine, a muscarinic receptor antagonist, by mecamylamine, a nicotinic receptor antagonist. Psychopharmacology (Berl). 2016;233(5):925-32.
28 Craig MC, Brammer M, Maki PM, Fletcher PC, Daly EM, Rymer J, et al. The interactive effect of acute ovarian suppression and the cholinergic system on visuospatial working memory in young women. Psychoneuroendocrinology. 2010;35(7):987-1000.

29 Craig MC, Fletcher PC, Daly EM, Rymer J, Brammer M, Giampietro V, et al. The interactive effect of the cholinergic system and acute ovarian suppression on the brain: an fMRI study. Horm Behav. 2009;55(1):41-9.
30 Grasby PM, Frith CD, Paulesu E, Friston KJ, Frackowiak RS, Dolan RJ. The effect of the muscarinic antagonist scopolamine on regional cerebral blood flow during the performance of a memory task. Exp Brain Res. 1995;104(2):337-48.
31 Sperling R, Greve D, Dale A, Killiany R, Holmes J, Rosas HD, et al. Functional MRI detection of pharmacologically induced memory impairment. Proceedings of the National Academy of Sciences of the United States of America. 2002;99(1):455-60.
32 Thienel R, Kellermann T, Schall U, Voss B, Reske M, Halfter S, et al. Muscarinic antagonist effects on executive control of attention. Int J Neuropsychopharmacol. 2009;12(10):1307-17.
33 Prohovnik I, Arnold SE, Smith G, Lucas LR. Physostigmine reversal of scopolamine-induced hypofrontality. Journal of cerebral blood flow and metabolism : official journal of the International Society of Cerebral Blood Flow and Metabolism. 1997;17(2):220-8.
34 Drevets WC, Zarate CA, Jr., Furey ML. Antidepressant effects of the muscarinic cholinergic receptor antagonist scopolamine: a review. Biol Psychiatry. 2013;73(12):1156-63.
35 Nagaoka T, Zhao F, Wang P, Harel N, Kennan RP, Ogawa S, et al. Increases in oxygen consumption without cerebral blood volume change during visual stimulation under hypotension condition. Journal of cerebral blood flow and metabolism : official journal of the International Society of Cerebral Blood Flow and Metabolism. 2006;26(8):1043-51.
36 Buccafusco JJ. The Revival of Scopolamine Reversal for the Assessment of Cognition-Enhancing Drugs. In: nd, Buccafusco JJ, editors. Methods of Behavior Analysis in Neuroscience. Boca Raton (FL); 2009.
37 Tapp PD, Chu Y, Araujo JA, Chiou JY, Head E, Milgram NW, et al. Effects of scopolamine challenge on regional cerebral blood volume. A pharmacological model to validate the use of contrast enhanced magnetic resonance imaging to assess cerebral blood volume in a canine model of aging. Prog Neuropsychopharmacol Biol Psychiatry. 2005;29(3):399-406.
38 Voss B, Thienel R, Reske M, Kellermann T, Sheldrick AJ, Halfter S, et al. Cholinergic blockade under working memory demands encountered by increased rehearsal strategies: evidence from fMRI in healthy subjects. Eur Arch Psychiatry Clin Neurosci. 2012;262(4):329-39.
39 de Celis Alonso B, Sergeyeva M, Brune K, Hess A. Lateralization of responses to vibrissal stimulation: connectivity and information integration in the rat sensory-motor cortex assessed with fMRI. NeuroImage. 2012;62(3):2101-9.
40 Masamoto K, Kim T, Fukuda M, Wang P, Kim SG. Relationship between neural, vascular, and BOLD signals in isoflurane-anesthetized rat somatosensory cortex. Cereb Cortex. 2007;17(4):942-50.

41 Alkire MT, Hudetz AG, Tononi G. Consciousness and anesthesia. Science. 2008;322(5903):876-80.
42 Hudetz AG, Wood JD, Kampine JP. Cholinergic reversal of isoflurane anesthesia in rats as measured by cross-approximate entropy of the electroencephalogram. Anesthesiology. 2003;99(5):1125-31.
43 Franks NP. General anaesthesia: from molecular targets to neuronal pathways of sleep and arousal. Nat Rev Neurosci. 2008;9(5):370-86.
44 Rudolph U, Antkowiak B. Molecular and neuronal substrates for general anaesthetics. Nat Rev Neurosci. 2004;5(9):709-20.
45 Tetrault S, Chever O, Sik A, Amzica F. Opening of the blood-brain barrier during isoflurane anaesthesia. Eur J Neurosci. 2008;28(7):1330-41.
46 Thal SC, Luh C, Schaible EV, Timaru-Kast R, Hedrich J, Luhmann HJ, et al. Volatile anesthetics influence blood-brain barrier integrity by modulation of tight junction protein expression in traumatic brain injury. PloS one. 2012;7(12):e50752.
47 Schwalm M, Schmid F, Wachsmuth L, Backhaus H, Kronfeld A, Aedo Jury F, et al. Cortex-wide BOLD fMRI activity reflects locally-recorded slow oscillation-associated calcium waves. Elife. 2017;6.
48 Burke M, Schwindt W, Ludwig U, Hennig J, Hoehn M. Facilitation of electric forepaw stimulation-induced somatosensory activation in rats by additional acoustic stimulation: an fMRI investigation. Magnetic resonance in medicine : official journal of the Society of Magnetic Resonance in Medicine / Society of Magnetic Resonance in Medicine. 2000;44(2):317-21.
49 Gruters KG, Groh JM. Sounds and beyond: multisensory and other non-auditory signals in the inferior colliculus. Front Neural Circuits. 2012;6:96.
50 Jain R, Shore S. External inferior colliculus integrates trigeminal and acoustic information: unit responses to trigeminal nucleus and acoustic stimulation in the guinea pig. Neuroscience letters. 2006;395(1):71-5.
51 Kessler M, Mamach M, Beutelmann R, Bankstahl JP, Bengel FM, Klump GM, et al. Activation in the auditory pathway of the gerbil studied with (18)F-FDG PET: effects of anesthesia. Brain Struct Funct. 2018;223(9):4293-305.

Table 1. Evoked activation differences in medetomidine-isoflurane combined anesthesia with GE EPI and SE EPI sequences (the size of blobs in mm^3 and the brain structures to which Z-score (pTFCE statistical inference, p=0.05 via GRF theory base FWER) peaks belong to). p. a. - stands for probable artefact, as our gradient echo images are not accurate enough around the cerebellum to firmly conclude the difference.

Exp. 2				
Treatment group	*EPI sequence*	*Size of pTFCE-wise blobs (mm^3)*		*Structures to which pTFCE-wise Z-score peak belongs to:*
		Uncorrected (3.1<z)	*Corrected (4.7<z)*	
Sal > SCO.	*GE*	14.2	7.3	L ECIC - Left external cx inferior colliculus
		5.1	-	R ECIC -Right external cx inferior colliculus
		4.0	0.01	L S1 BF - Left primary somatosensory cortex, barrel field
		0.1	-	Left cerebellar lobe (p.a.)
	SE	0.02	-	L S1 BF - Left primary somatosensory cortex, barrel field
Sal > BSCO	*GE*	33.6	13.3	L ECIC - Left external cortex inferior colliculus
	SE	-	-	-
Sal > DON	*GE*	20.8	-	Left cerebellar lobe (inferior colliculus)
	SE	-	-	-
SCO > Sal	*GE*	4.0	0.2	Left cerebellar lobe
		0.3	-	Right cerebellar lobe (p.a.)
		0.2	-	Right cerebellar lobe (p.a.)
	SE	0.3	-	L S1 J primary somatosensory cortex, jaw region
		0.3	-	VPM –ventral posteromed thalamic nucleus
SCO > BSCO	*GE*	0.8	-	L cerebellar lobes (p.a.)
	SE	-	-	-
SCO > DON	*GE*	3.1	-	Right cerebellar lobes -Crus2
		0.2	-	Left Cerebellar lobes (p.a.)
		0.1	-	L VTg – Left ventral tegmental nucleus
	SE	0.2	-	R PrS - Right presubiculum
BSCO > SCO	*GE*	5.9	0.5	L S1 BF – Left primary somatosensory cortex, barrel field
	SE	0.02	0.01	L S1 BF – Left primary somatosensory cortex, barrel field
BSCO > Sal	*GE*	5.2	-	L Cerebellar lobe
	SE		-	
DON > SAL	*GE*	-	-	-
	SE	1.1	-	L S1ULp – Left primary somatosensory cortex, upper lip
		0.1	-	L S1 BF – Left primary somatosensory cortex, barrel field
DON > SCO	*GE*	6.8	1.8	R ECIC – Right external cx inferior colliculus
	SE	2.2	0.01	L S1 BF primary somatosensory cortex, barrel field
DON > BSCO	*GE*	7.0	1.8	R ECIC - Right external cortex of inferior colliculus)
		2.1	-	Right cerebellar lobes (p.a.)
	SE	0.1	0.01	L S1 BF – Left primary somatosensory cortex, barrel field